The Potential of Utilizing Geothermal Energy Coupled with Geomechanics: A Case Study for Trinidad and Tobago

Justin Bell-Eversley* [iD] , Chandra Ramnath* [iD] , David Alexander* [iD] , Rean Maharaj**‡ [iD] , Donnie Boodlal** [iD]

*Energy Systems Engineering Unit, University of Trinidad & Tobago, Esperanza Road, Point Lisas, Trinidad & Tobago

**Process Engineering Unit, University of Trinidad & Tobago, Esperanza Road, Point Lisas, Trinidad & Tobago

‡ Corresponding Author; Rean Maharaj, Esperanza Road, Point Lisas, Trinidad & Tobago, Tel: +1 868 642 8888, rean.maharaj@utt.edu.tt

Abstract- Trinidad and Tobago (TT), a small island developing state (SIDS), has been experiencing the impact of global warming and climate change. TT has been heavily dependent on fossil fuels and has been lagging behind the rest of the Caribbean in transitioning to utilizing green energy. This paper focused on the evaluation of the potential for harnessing geothermal energy from a conceptual reservoir using field data and utilizing the commercial software CMG. The Upper Cruse sand in the Parrylands area was selected since there was geothermal potential due to its proximity to mud volcanoes and high geothermal gradients. The impact of rock geomechanics was also investigated. The results for the single porosity models which were developed showed that an optimum cumulative enthalpy of 5.507E+12 Btu was achieved at a constant water reinjection pressure of 1000 psi with a well spacing of 1300 ft. Using two-way coupling and the same parameters of this optimum case, a geomechanical analysis of the Natural Fracture (3D Linear Elastic) Geomechanical Model gave an enthalpy of 4.187E+12 Btu. These results coincided with a reduction in CO2 emissions of 1043.07 MM lbs when compared to using natural gas for the generation of electricity. In addition, when the unsubsidized electricity price of US$ 0.35 was used in the economic evaluation, the associated IRR was 39.2%. This study demonstrated the significant potential of geothermal energy as a sustainable substitute for natural gas for the generation of electricity in TT.

Keywords geothermal energy, geomechanical analysis, natural fractures, climate change, economic evaluation.

1. Introduction

One of the most significant threats globally is climate change. A significant and increasing amount of anthropogenic CO_2 generated by countries is entering the atmosphere (Fig.1) and is contributing significantly to global warming. Activities such as the burning of fossil fuels, trap heat within the earth's atmosphere, raising global temperatures. World Bank statistics in 2019 showed that Trinidad & Tobago (TT) is ranked 2nd in the world in carbon dioxide emissions per capita [1].
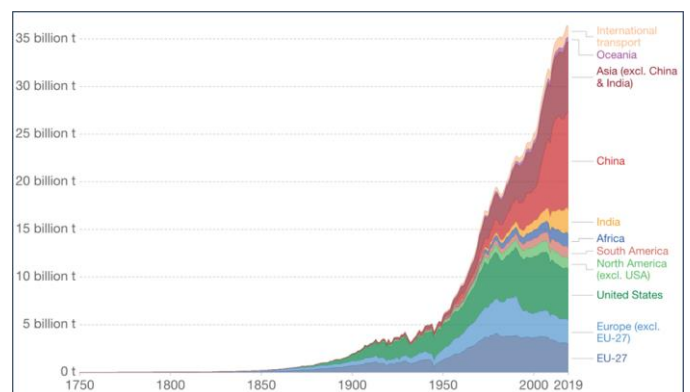

Fig. 1. CO_2 Emissions by World Region from 1750 To 2019 [2].

As the world's population grows, the increase in consumption of energy is one of several factors responsible for the increase in greenhouse gas emissions. Figure 2 below shows the historical and projected world energy consumption, where primary energy consumed from fossil fuel sources is forecasted to increase, leading to a continuous rise in carbon dioxide emissions worldwide [3]. In fact, CO_2 accounts for 76% of the world's anthropogenic emissions [4].

The twin island Republic of Trinidad and Tobago, located to the south of the Caribbean, has benefited greatly from its fossil fuel reserves. Commercial oil production started near the country's Pitch Lake in 1908 and still continues today. TT has a high dependency on the oil and natural gas sector which accounts for 85 percent of total export earnings, 40 percent of government revenue, and over 35 percent of Gross Domestic Value [5]. TT is affected by depleting resources and its oil production has also been declining from 114.257 thousand bbl/day in 2008 to 58.904 thousand bbl/day in 2019 as shown in Figure 3 [6]. The global energy crisis, enhanced global warming and environmental pollution have become main drivers in the selection of the source of energy and renewables have become established as mainstream sources of energy [7]. As a main part of primary energy, crude oil shall certainly be affected deeply by renewable energy sources in the future. Diversification of this country's energy mix has been a topic of greater interest in recent years and more attention has been given to alternative means of energy generation. As a result, and in keeping with the Paris Agreement [8], TT needs to investigate the potential use of other cleaner sources of energy consistent with
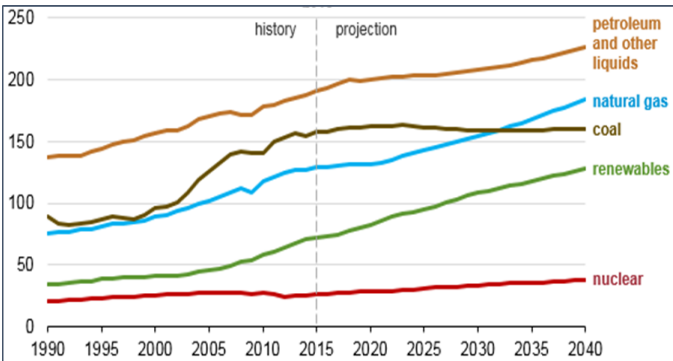
strategic decisions and policies adopted by other countries around the world [9-12].

Historically TT's government has been able to provide its population with heavily subsidized fuel [13]. The eventual removal of these subsidies will create a need for diversification of the current energy mix and development of alternative sources of energy. Geothermal energy is considered to be a reliable source of energy since it is independent of weather conditions, unlike other renewable energy sources such as solar and wind. It can create revenue through taxation and is also capable of "supplying baseload electricity and providing ancillary services for long-term periods" [14, 15].

Geothermal energy in the Caribbean is derived from volcanic activity that supplies energy for geothermal reservoirs. Available research indicates that many countries within the Caribbean have shown great potential for geothermal energy. Although the capability for geothermal energy is undeniably evident in the Lesser Antilles, there isn't current evidence of geothermal reservoirs present in TT. However, potential evidence for harnessing geothermal energy arises due to the existence of geothermal hotspots with temperature gradients of 32°C/km, exceeding the average geothermal gradient for this country of 20-23°C/km [16, 17]. Mud volcanoes located in the southern area of the country and varying geothermal gradients established by Deville & Guerlais [18] also show evidence towards this country's potential thermal capabilities (Fig.4).
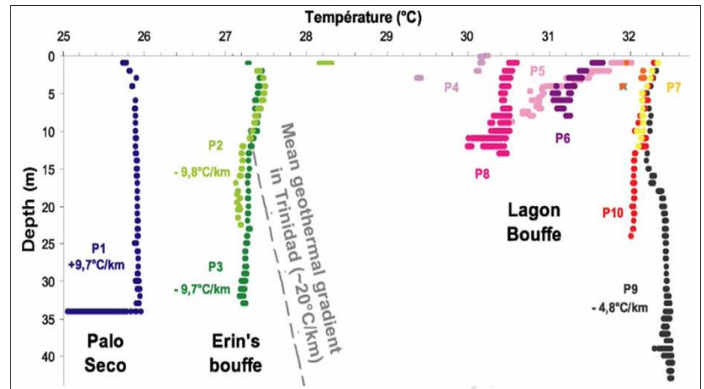

Fig. 2. World Energy Consumption by Energy Source from 1990-2040 [3].
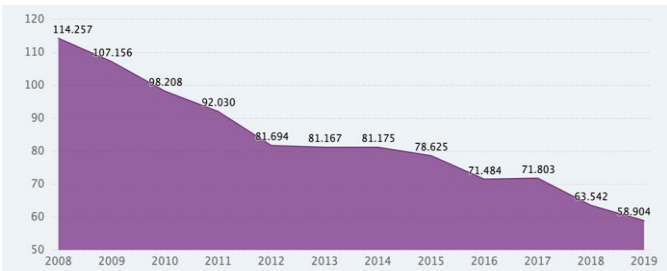
Fig. 3. Trinidad and Tobago's Crude Oil Production from 1960 to 2019 [6].

Fig. 4. Different Temperature Profiles Recorded in Conduits of Several Mud Volcanoes in Trinidad [18]

This study would investigate the potential capabilities for using geothermal energy in TT using a hypothetical model based on practical field data (from the Parrylands Area) seeking to quantify the amount of energy that can be produced from these reservoirs. Other major objectives would be to construct single porosity and natural fracture dual permeability models along with testing sensitivity scenarios using CMOST. Water reinjection and well spacing would be investigated to optimize energy production. This paper also seeks to examine the geomechanics of the reservoir, where the production of fluid from the reservoir affects fluid flow due to deformation. These investigations include a feasibility analysis to be conducted along with the determination of

reduced net CO_2 emissions from using geothermal energy when compared to energy derived from fossil fuel sources.

2. Methodology

Figure 5 illustrates the activities involved in the execution of this study.

2.1. Geological Setting

Through qualitative and quantitative methods, most of the data collected were obtained from secondary sources. Data for input values were obtained from correlations made from fields similar to our field of interest located in the Parrylands Area in south western Trinidad (Fig.6).

Steam flooding projects were performed historically in this field, and its reservoir comprises of Cruse 'E' Sands lying "north of the Los Bajos fault system along the northern flank of the east-west trending Point Fortin anticline feature" [19]. The Cruse Formation is Late Miocene to Early Pliocene in age and comprises of sandstones, claystones, and siltstones, with deposits from the basin floor and slope fan deposits. The Upper Cruse is predominantly dark grey, non-.

Fig. 6. Parrylands Area Where Steamflooding Was Performed [19]

calcareous shale with irregular nodules of hard grey claystone. The Lower Cruse is dominated by grey to black, gypsiferous clays that weather brownish-yellow to red with interspersed silty clays, silts and sandstone units which coarsen upward into the thick sandstone units of the Upper Cruse [20]. According to Ramlal [19], the thick shale of the Lower
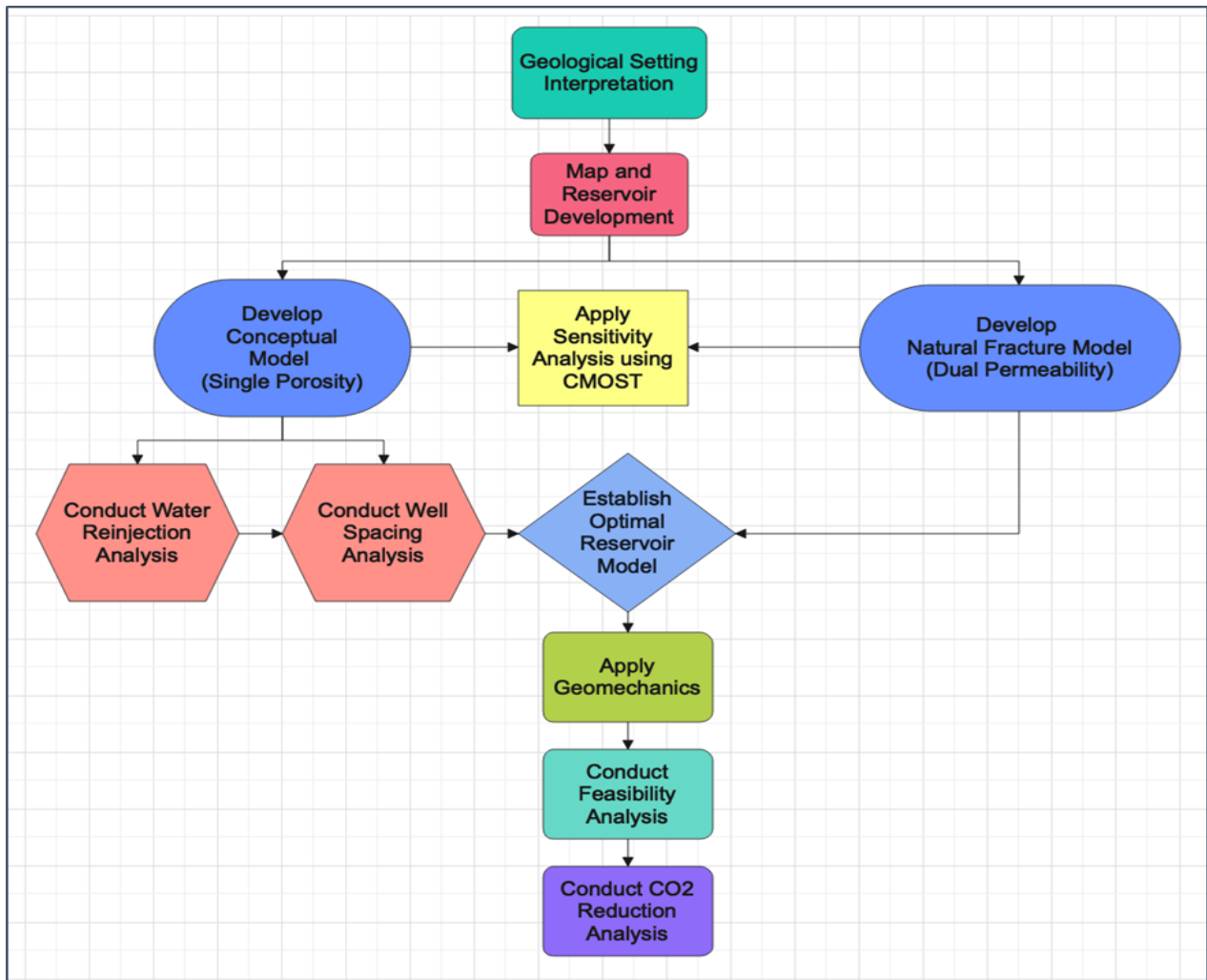

Fig. 5. Roadmap methodology

Forest clay overlies the Cruse sands. These sand units consist of north-east/south-west trending distributary channel/mouth bar complexes, which were deposited in a lower deltaic plain environment. Well log data obtained from the field (Fig.7) shows that not only is there good sand development, especially in units B and C, but that these reservoirs are separated by very distinct shale units. This information was taken into consideration in the development of our geothermal models.

2.2. Map and Reservoir Development

Didger and the CMG software were utilized to develop & digitize the structure map and geothermal reservoir models respectively. The contours for the structure map and the net oil sand isopach maps, which were retrieved from a study done by Ramlal [19] on the Parrylands Area, were digitized for the development of our reservoir. This allows for a more accurate assessment of the volumetrics of the reservoir. The well type log (Fig.7) shows 7 distinct layers, comprising of sand and interbedded shale which aided in the development of the reservoir model. This information allowed for thicknesses of sand and shale units to be measured and inputted into CMG software for model development. We assumed that faults within the reservoir were non-sealing, since this particular characteristic was not specified in any of the literature that we were able to access. Table 1 shows the parameters specific to the Parrylands Area.

The static model illustrated in Fig.8 shows the differentiation between sand and interbedded shale.

2.3. Conceptual Model (Single Porosity)

This conceptual model was designed to determine the viability of a geothermal field in TT using practical field data. Even though TT has not yet found any geothermal reservoirs
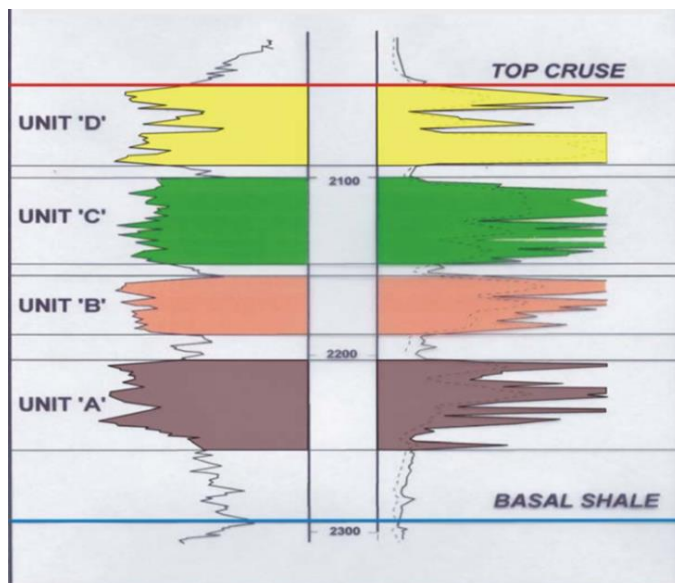

Fig. 7. Well Log Data Obtained in Cruse Sands [19]

within its boundaries, this research can be utilized to understand and predict the performance of geothermal reservoirs with similar geologic and reservoir properties, once identified. The temperature was calculated based on the assumption that this hypothetical geothermal reservoir is in the vicinity of an actual geothermal hotspot in Trinidad, which was mentioned to have geothermal gradients of up to 32°C/km [16]. According to a publication by IRENA [21], for a binary plant that is able to utilize lower temperature fluids between the range of 212 - 338°F (100 - 170°C), when the fluid temperature is lower than 212°F, electrical energy output efficiencies tend to decrease greatly. Therefore, a base case reservoir temperature of 212°F (100°C) was selected as temperatures below this are unlikely to be viable or are inefficient in some cases.

Table 1. Parameters used in geothermal model [19].

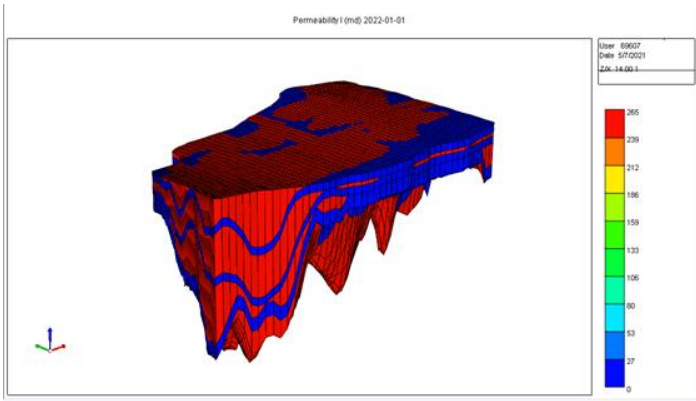| Parameter	Value
Depth to Top of Sand	2050ft
Permeability	265mD
Porosity	31%
Sand Thickness	75ft

Fig. 8. Visual Representation of the Reservoir Model's Sand and Shale distribution

The lower limit reservoir temperature (114.8°F) was calculated to be the temperature of the actual reservoir, at a depth of 2050ft. To satisfy the required temperature gradient (32°C/km) and in order to achieve temperatures of 212°F (100°C), reservoirs have to be drilled to at least 7500ft. The thermal properties requirements outlined by Chekhonin et al. [22] and shown in Table 2 are applicable for sandstone which is applicable to the nature of TT's reservoirs. Component values were attained using data retrieved specifically for water [23].

Data from Villaluz [24] which determined the relative permeability in the Berea sandstone, was used to correlate the reservoirs containing sandstone in our area of interest. The relative permeability utilized for this team's models from the Berea Sandstone is illustrated in Figure 9.

The viscosity data used was obtained from the viscosity of water at a constant pressure of 1000 psi which was the approximate pressure expected in the Parrylands reservoir. This viscosity data was provided at varying temperatures that were critical to geothermal reservoir development. The values attained are shown in Figure 10.
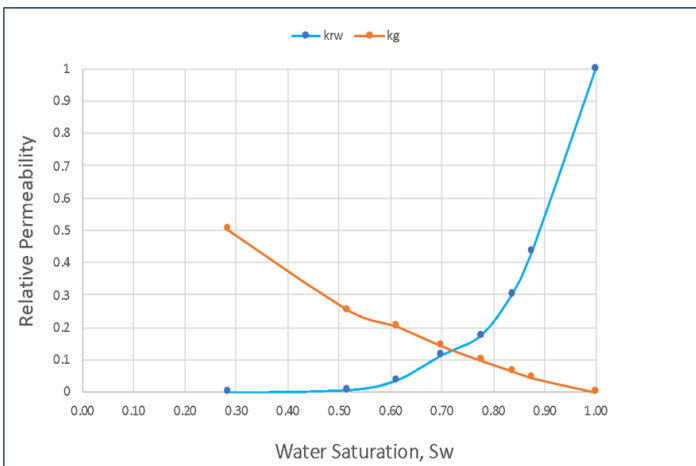

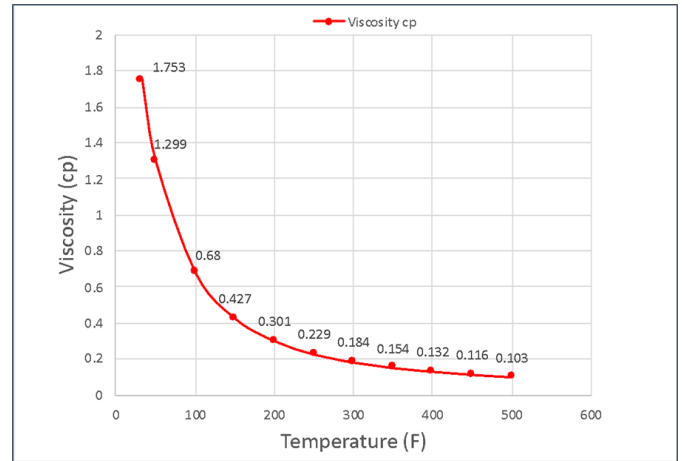**Fig. 9.** Relative Permeability of Berea Sandstone Used in our Models (Villaluz, 2005).

Fig. 10. Viscosity of Water at a Constant Pressure of 1000 psi with varying Temperature

2.4. Natural Fractures

Natural fracture modelling was used to investigate the possible energy production outcomes, when natural fractures are inputted into the reservoir, as opposed to a single porosity, homogeneous situation. Porosity models with natural fractures were developed for comparison with a base case without fractures, in order to observe the performance of reservoirs. The range of data used for this study is outlined in Table 3. The natural fractures model requires that a relative permeability be defined for two rock types. For the first rock type, the relative permeability of the Berea sandstone (Fig.9) was used for the matrix. For rock type 2, relative permeability has to be relative to the fracture where the values used can be defined, as seen in Table 4.

2.5. Geomechanics

Geomechanics was applied to the models to enhance the accuracy of data forecasting by accounting for variations in pore pressure, porosities, permeabilities, and overall reservoir volumetrics as the reservoir deforms due to variations in stresses and strains causing compaction and/or subsidence. Two-Way Coupling was incorporated in this study so that deformation experienced within the simulation run could have an effect on the fluid flow due to the new pore compressibility, new porosity and absolute permeability transferred to the simulator [25].

Three types of geomechanics were applied to both the conceptual and natural fractures models in this study: Linear Elastic, Non-Linear Elastic, and Elasto-Plastic, incorporating the Mohr Coulomb and the Drucker-Prager models. These were used to investigate the effect of deformation on enthalpy production. Three different Linear Elastic approaches were used, inputting a relatively large cohesion value, so that no yield could occur and allowing the model to be purely elastic. Parameters for the 3D Simple Linear Elastic model were obtained from a paper by Xu et al. [26], where they examined geomechanical properties of sandstone that allowed for correlations to be made to our

Table 2. Parameters used in developing conceptual single porosity model.

Section	Parameters	Lower Limit	Base Case	Upper Limit	Unit
Reservoir	Temperature	114.8	212	302	°F
	Matrix Porosity	0.22	0.31	0.38	%
	Permeability I	198.75	265	331.25	mD
	Permeability J	198.75	265	331.25	
	Permeability K	19.88	26.5	33.13	
	Rock Compressibility	3.0403e-6	3.0403e-6	3.0403e-6	1/psi
	Reservoir Pressure	857.907	953.25	1048.575	psi
Thermal	Volumetric Heat Capacity	14.91066	37.2767	59.6427	Btu/(ft3*°F)
	Thermal Conductivity Rock	6.9379	48.5666	90.19536	Btu/(ft*day*°F)
	Thermal Conductivity Water	8.33	8.33	8.33	Btu/(ft*day* °F)
Components	Critical Temperature	705.038	705.038	705.038	°F
	Liquid Compressibility	5.0e-6	5.0e-6	5.0e-6	1/psi
	Molar Density	3.4637	3.4637	3.4637	lbmole/ft^3
	Molecular Weight	18.02	18.02	18.02	lb/lbmole
	1st thermal expansion	0.000695	0.000695	0.000695	1/F

reservoir in TT. The Simple 2D Plain Strain Approach was also used. The parameters used in both approaches are shown in Table 5.

Table 6 gives the parameters used in the Pseudo-Dilation Option where variations in Young's Modulus at different threshold pressures aid in determining the change in porosity from the applied stresses and strains. Here, a smaller Young's Modulus value tends to make the materials more elastic and more deformable [27].

The purpose of implementing the Hypoelastic and Hyperelastic models was to portray a Non-Linear Elastic model to simulate the impact of modifying the Bulk and Shear Modula and Poisson's ratio in the elastic region. The previous model input values for Young's Modulus and Poisson's ratio were reused from the 3D Linear Elastic Case. However, new parameters for the hypoelastic case were implemented (Table 7). Similar data were used in the hyperelastic case but with additional parameters.

Most of the parameters in Table 5 were also used in the Mohr-Coulomb and Drucker-Prager Elasto Plastic Models. However, the major difference the cohesion value of 36.26 psi, reduced from 2030.53 to allow for failure to occur within the reservoir.

3. Results & Discussion

3.1. Conceptual Model Single Porosity

3.1.1. CMOST Sensitivity Analysis

Upper and lower limit parameters were set for the single porosity model (Table 2), where values could be tested against various scenarios. For this sensitivity analysis to be done, results for the base case scenario, using base case parameters in the same table, first had to be generated. Figure 11 shows the results of the cumulative enthalpy production

Table 3. Parameters used in Natural Fracture Models.

Section	Parameters	Lower Limit	Base Case	Upper Limit	Unit
Reservoir	Temperature	114.8	212	302	°F
	Fracture Temperature	114.8	212	302	
	Matrix Porosity	0.22	0.31	0.38	%
	Fracture Porosity	0.0054	0.006	0.0066	
	Permeability I	198.75	265	331.25	mD
	Permeability J	198.75	265	331.25	
	Permeability K	19.88	26.5	33.13	
	Fracture Permeability I	1987.5	2650	3312.5	mD
	Fracture Permeability J	1987.5	2650	3312.5	
	Fracture Permeability K	198.75	265	331.25	
	Fracture Spacing I	29.52756	32.8084	36.08924	ft
	Fracture Spacing J	29.52756	32.8084	36.08924	
	Fracture Spacing K	0	0	0	
Thermal	Rock Compressibility	3.0403e-6	3.0403e-6	3.0403e-6	1/psi
	Porosity Reference Pressure	857.907	953.25	1048.575	psi
	Volumetric Heat Capacity	14.91066	37.2767	59.6427	Btu/(ft3*oF)
	Thermal Conductivity Rock	6.9379	48.5666	90.19536	Btu/(ft*day*°F)
	Thermal Conductivity Water	8.33	8.33	8.33	Btu/(ft*day*°F)
Components	Critical Temperature	705.038	705.038	705.038	°F
	Liquid Compressibility	5.0e-6	5.0e-6	5.0e-6	1/psi
	Molar Density	3.4637	3.4637	3.4637	lbmole/ft3
	Molecular Weight	18.02	18.02	18.02	lb/lbmole
	1st thermal expansion	0.000695	0.000695	0.000695	1/F

Table 4. Permeability Assigned to the Fracture in Natural Fracture Model.

Sw	krw	krow
0.01	0	1
0.99	1	0

Table 5. Parameters used in Simple 3D Elastic Model retrieved from [26].

Parameters	Unit	Values
Young's Elastic Modulus	psi	5,273,572
Poisson Ratio	ratio	0.272
Cohesion	psi	2030.53
Confining Pressure	psi	4641.21

Table 6. Data used in Pseudo Dilation Model.

Parameters		Unit	Values
	Young's Elastic Modulus	psi	5,273,572.1
	Poisson Ratio	ratio	0.272
Dilation state:	Threshold Pressure	psi	1400
	Young's Modulus	psi	7987
Recompaction state:	Threshold Pressure	psi	400
	Young's Modulus	psi	19099.9

Table 7. Parameters used in Hypoelastic Case.

Parameters	Unit	Values
Young's Elastic Modulus	psi	5,273,572
Poisson Ratio	ratio	0.272
Coefficient Modulus (for Bulk Modulus)	psi	2030.53
Exponential Power (Defines Non-Linerarity of Bulk Modulus)	decimal	0.4

from the entire field model, including 6 producer wells and 6 water re-injectors. The black line represents the base case cumulated enthalpy after 28 years from the start of production in year 2022, up until 2050. The enthalpy cumulated was approximately 4.7×10^{12} Btu. The lowest and highest expected results, when parameters were varied within the limits set, were approximately 1.4×10^{12} Btu and 7.7×10^{12} Btu respectively, over 28 years. The enthalpy rates shown in Figure 12 reflect trends where the majority of the sensitivity graphs generated after 2040 experienced a drop in rate of enthalpy which could have resulted from a variety of situations. One of these scenarios would occur when the injection pressure is not able to pressurize the formation as good as it once did. CMOST gives important information as to what parameters tend to have the most impact on production of enthalpy based on the parameters set.
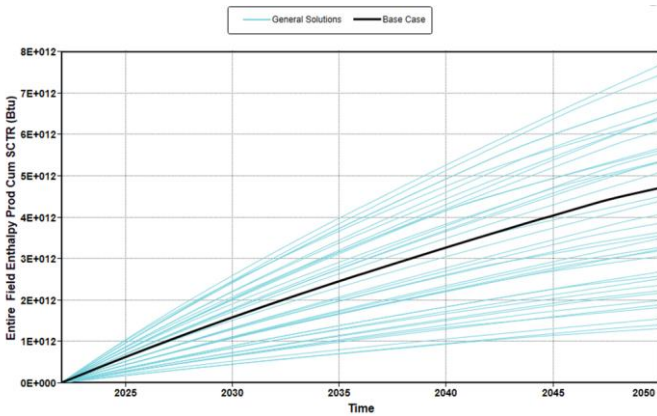
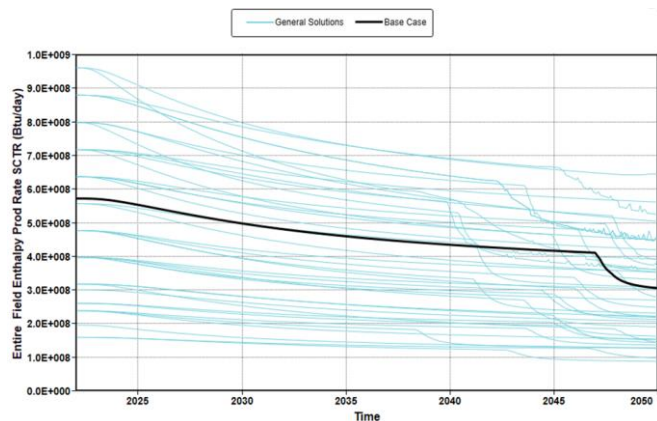**Fig. 11.** Field Cumulative Enthalpy Over 28 Years

Fig. 12. Field Enthalpy Rates Over 28 Years

Further investigation showed that the temperature of the reservoir had the greatest effect on enthalpy produced in the field, which aids in determining the amount of power that could be generated from this conceptual geothermal model. A paper by IRENA [21] showed that temperatures below 212°F (100°C) tend to contribute to a decrease in electrical energy output efficiencies. It was therefore assumed that even though geothermal power plants could operate at lower temperatures, the chosen benchmark for surface production would need to be in the vicinity of 212°F (100°C) for optimal performance. The temperature downhole in the sensitivity analysis shows that below the base case scenario, temperature tends to fall below the 212°F (100°C) benchmark. It was also found that the fluid temperature decreased as it was brought to the surface from downhole, which creates the assumption that this reduction was due to heat energy losses attained as the heated fluid flowed up the tubing.

3.1.2. *Water Reinjection Analysis*

Water re-injection was used in maintaining good reservoir pressure so that the geothermal power plant could produce energy that is sustainable over a long period of time. To set up a suitable water reinjection program, the effect of different water injection pressures on our conceptual single porosity geothermal model was tested. The pressures that were investigated were 1350 psi, 1000 psi and 500 psi. The fracture pressure of the reservoir was calculated using a fracture pressure gradient of 0.7 psi/ft, then multiplying that value by the depth to the top of the sand (2050 ft), giving a fracture pressure of 1435 psi. It was ensured that the highest reinjected pressure was at least 85 psi less than the fracture pressure, as a safety measure. The reinjection pressures were determined to ensure pressure injected would not fracture the reservoir and compromise the credibility of the results. It was observed that as the water injection rate increases, the downhole temperature drops at a faster rate.

In Figure 13, for the smallest injection pressure of 500 psi, in the base and upper limit case, in year 2036 and 2048 respectively, the cumulative enthalpy began to decrease below cumulative enthalpy for the higher injection pressures (1000 psi and 1350 psi). This seemed to occur due to the reservoir not being pressurized effectively for the injection pressure of 500 psi, when compared to higher injection pressures for the base and upper limit case. In Figure 14, there is a major decrease in enthalpy rate for injection pressure of 500 psi. This occurrence is due to the inability of the injection pressure to sustain the reservoir pressure after a certain time when compared to higher injection pressure scenarios which are able to sustain reservoir pressure and enthalpy over a longer period of time.
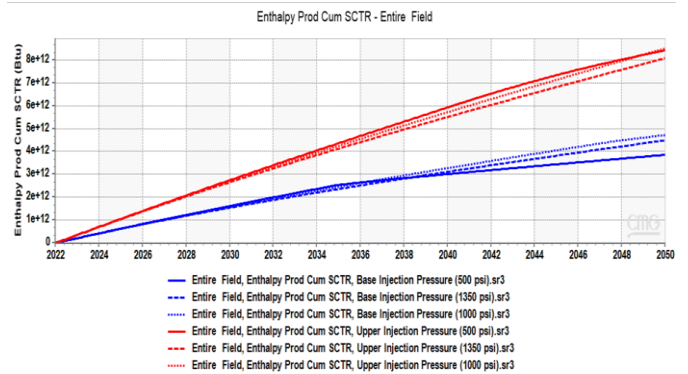

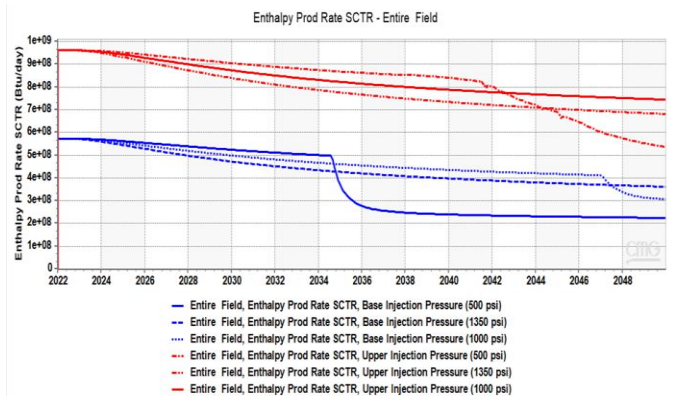**Fig. 13.** Cumulative Enthalpy Produced for Different Injection Pressures

Fig. 14. Forecasted Enthalpy Rate for Different Injection Pressures of the Conceptual Model

3.1.3. Well Spacing Analysis

In this study, the effect of well spacing between producers and injectors for all wells was looked at. The investigation was done by varying different well spacing at a constant injection pressure of 1350psi. In Figure 15, well spacing from 250ft to 1300ft were initially investigated which demonstrated that an increase in well spacing led to an increase in cumulative enthalpy. This direct relationship between well spacing and cumulative enthalpy is maintained as well spacing increases. This is because the injected water, at a constant pressure, has more time to exchange heat with the formation, as it flows towards the producer. The closer the injector well is to the producer, the more the enthalpy decreases due to the water having shorter travelling times as it makes its way towards the producer wells, limiting the time for heat exchange and for water to absorb energy. This direct relationship between well spacing and the production of cumulative enthalpy comes with its limitations.

It was observed that at a particular distance between injector and producer, the rate at which cumulative production enthalpy increased began to slow as well spacing increased. Figure 16, which incorporated an additional data
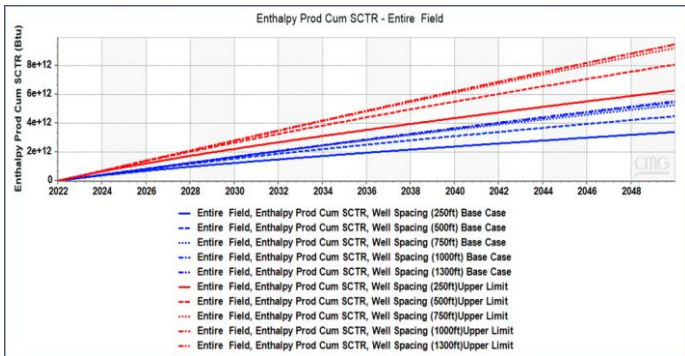

Fig. 15. Cumulative Enthalpy Production for Various Well Spacing for Base Case and Upper Limit Case Scenario

Fig. 16. Enthalpy Cumulative Production at Various Well Spacings for a 28-year period for Base and Upper Limit Case at Constant Injection Pressures of 1350psi, 1000psi and 500psi

point for well spacing of 1500ft, illustrates this entire phenomenon. It can be seen for all graphs (with the exception of the graph with the constant injection pressure of 500psi), that after the well spacing of 750ft, there was a drastic shift in gradient of the graph, leading to the assumption that the positive effect of increased well spacing was reduced. After the graphs plateaued, they began to dip, showing a decrease in cumulative enthalpy production after the well spacing of 1300 ft. This led to the assumption that enthalpy cumulative production would begin to decrease at well spacings in excess of 1300ft, due to the inability of water injected to affect producers, provide proper pressure maintenance of the field, and establish an effective link with producers as a result of the large well spacings. This decrease in enthalpy occurred for well spacing between the range 1300ft to 1500ft. Further analysis shows that at a constant injection pressure of 1000psi, produced the highest cumulative enthalpy over the 28 years.

As shown in Figure 16 depicting the results of the well spacing analysis, the cumulative enthalpy for water being injected at a constant pressure of 1000psi produced more enthalpy to be produced over the span of 28 years. These sensitivity analyses were performed on the conceptual single porosity model, the results which will also be used to determine the optimized strategy within the project.

Analysis was also done on well spacing, where a constant injection pressure of 500psi was applied to the model, to investigate the expected changes to enthalpy if the constant injection pressure is reduced further. Figure 16 shows that for a constant injection pressure of 500psi, the majority of the cumulative enthalpy values are less than the values for other constant injection pressures. The upper-case values show that after the well spacing of 250ft for the constant injection pressure of 500psi, the enthalpy began to decrease drastically below the other higher injection pressure values. It is believed that due to the injection pressure (500psi) being relatively low, as the well spacing increases the reservoir is not able to be pressurized as well as the scenarios with higher injection pressures.

3.2. Natural Fractures (Dual-Permeability)

3.2.1. CMOST Sensitivity Analysis

The results in Figure 17 show that temperature also had a major effect on enthalpy produced for the entire field (6.883E+12) when ranged between temperatures of 114.8°F to 302°F (Table 3). The maximum enthalpy produced for the entire field can reach limits of 8.259E+12 Btu of energy. The results reflected in Figure 18 show that the enthalpy produced within the lower and upper limits allowed for decent energy production. Establishing values above the base case scenario would be favorable as the conceptual geothermal power plant would be able to run as efficiently and as steadily as possible.
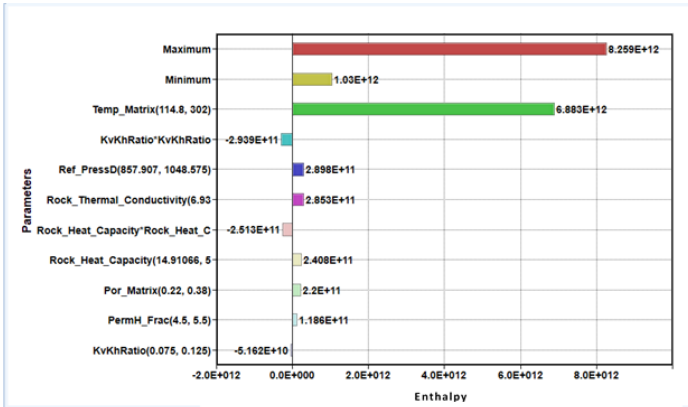
Fig. 17. The Effect of Various Parameters on Enthalpy Produced for the Field

3.2.2. Geomechanical Analysis

Results reflected in Figures 19 and 20, show that when Linear 3D geomechanics is added to both the conceptual single porosity and the natural fractures models, the values decrease when compared to the models without geomechanics applied. When 3D Linear Elastic models are incorporated, the cumulative enthalpy throughout the years decreased to 4.159E+12 Btu and 4.221E+12 Btu respectively.

With respect to the Linear Elastic models (3D, 2D and Pseudo Dilation), Non-Linear Elastic (Hypoelastic and Hyperelastic) and Elasto Plastic (Mohr-Coulomb and Drucker-Prager), a decrease in enthalpy is experienced when geomechanics is applied. This result can be seen for all models in Table 8.

3.3. Feasibility Study

This study sought to examine the implementation of a conceptual geothermal model along with the determination of its economic viability. A feasibility analysis of the project was conducted and analyzed with regard to the natural fractures model incorporating geomechanics (Simple 3D Linear Elastic). This model was optimized, incorporating a well spacing of 1300ft and a constant reinjection pressure of

Fig. 18. Results for Enthalpy Produced Cumulated

1000psi. The results obtained for this model tend to be closer to what would be expected to occur in a reservoir, as opposed to utilizing a single porosity model which does not contain natural fractures. The economic analysis explored the financial capabilities, cost, and overall feasibility of engaging in a conceptual geothermal project, incorporating values which could pertain to Trinidad and Tobago where possible. One of the most important criteria obtained at the start of the feasibility analysis was the potential power that could be generated from the energy/enthalpy produced over a 28-year period. Results are seen in Table 9.

Since 1 J/s is equivalent to 1 Watt, the enthalpy expressed in British thermal units (Btu) had to be converted to Joules, then to Joules per second, by dividing cumulative enthalpy by 883,008,000 seconds (28years). Power in Megawatts could then be calculated. This potential power in Megawatts, was then used to determine potential capital expenditure of a binary geothermal power plant. Since the relatively low temperatures that exist in these models cannot sustain any other type of geothermal power plants, such as flash and dry steam systems, the binary geothermal plant was selected. The capital expenditure values within the minimum, likeliest and maximum sections in Table 10, were obtained
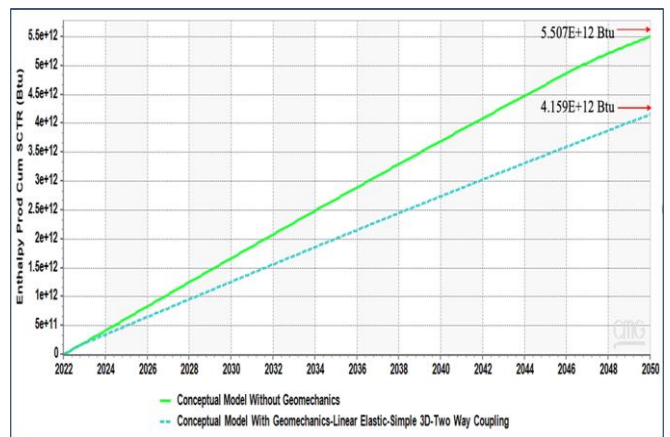

Fig. 19. Cumulative Enthalpy for Single Porosity Model With and Without Geomechanics. (Simple 3D Linear Elastic Two Way Coupling)
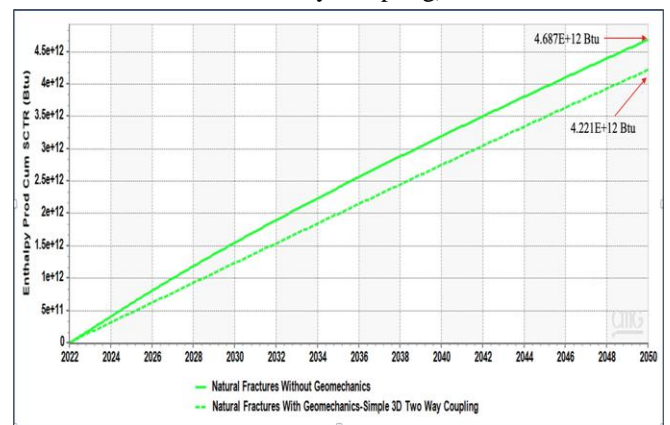

Fig. 20. Cumulative Enthalpy for Natural Fractures Model with and without Geomechanics. (Simple 3D Linear Elastic Two Way Coupling)
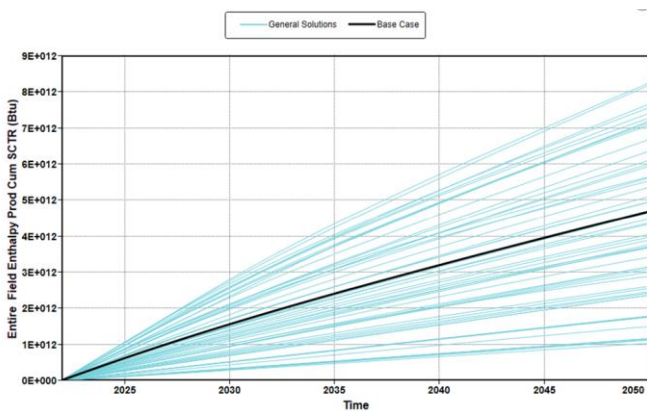
Table 8. Results from Geomechanical Analysis.

LINEAR ELASTIC	
Conceptual (Single Porosity)	**Cumulative Enthalpy for 28 Years (Btu)**
Without Geomechanics	5.507E+12
3D	4.159E+12
2D	4.144E+12
Pseudo Dilation	4.1586E+12
Natural Fracture (Dual Permeability)	**Cumulative Enthalpy for 28 Years (Btu)**
Without Geomechanics	5.581E+12
3D	4.187E+12
2D	4.162E+12
Pseudo Dilation	4.183E+12
NON-LINEAR ELASTIC	
Natural Fracture (Dual Permeability)	**Cumulative Enthalpy for 28 Years (Btu)**
Hypoelastic	4.282E+12
Hyperelastic	4.332E+12
ELASTO PLASTIC	
Conceptual (Single Porosity)	**Cumulative Enthalpy for 28 Years (Btu)**
Mohr-Coulomb	4.159E+12
Drucker-Prager	4.159E+12
Natural Fracture (Dual Permeability)	**Cumulative Enthalpy for 28 Years (Btu)**
Mohr-Coulomb	4.176E+12
Drucker-Prager	4.170E+12

Table 9. Values Used to Calculate Power Potential in Natural Fractures Model Incorporating Geomechanics (Simple 3D Linear Elastic Case-Mohr-Coulomb)

from two sources: one from a briefing by the International Renewable Energy Agency [21], and the second from a paper done by the U.S. Energy Information Administration on Capital Cost [28]. The operating costs for geothermal systems are relatively small and these values were obtained from an online publication produced by the Office of Energy Efficiency and Renewable Energy [29].

The revenue expected to be generated from the geothermal model is dependent on the price that citizens pay to the Trinidad and Tobago Electricity Commission (T&TEC) which is presently heavily subsidized. A recent (2021) bill received from T&TEC states that for the first 400 kWh and the next 600 kWh of energy used, the cost is TT 0.26 cents and TT 0.32cents per kWh respectively. These values were used in the minimum and likeliest sections in Table 10. Given that the cost of electricity in T&T is heavily subsidized when compared to other countries, the maximum value used for revenue of the geothermal project was obtained from a thermo-economic analysis done on a binary power plant in Indonesia which had a revenue of US$0.083/kWh.

The base economic results for this paper were calculated based on the parameters used under the likeliest section of Table 10. This was done to determine when payback would occur, what would be the Net Present Value (NPV) of the project using a minimum acceptable rate of return of 10% , and the expected Internal Rate of Return (IRR) of the project. The results from the economic evaluation are reflected in Table 11.

Table 11 shows the payback period ending in 2042 if the project were to begin production in 2022, materializing after approximately 20 years. The project, according to the results, would have a return on investment of 2.7% which is below the minimum acceptable rate of return of 10%. The NPV also illustrates that the project would not be feasible based on the input parameters used from the likeliest section in Table 10. Further investigations were done for a more in-depth analysis of the project via a sensitivity analysis using the Crystal Ball Software to conduct Monte Carlo simulations. This allowed for capital expenditure, operating cost, and revenue to be defined within a range, where the software could vary the selected parameters and simultaneously give insight as to how those parameters affect NPV and IRR. In running

Time of Production (Years)	Cumulative Enthalpy Produced (Btu)	Cumulative Enthalpy Produced (J)	Cumulative Enthalpy Produced (90% Efficiency) (J)	J/s	Power (MW)
28	4.19E+12	4.42E+15	3.98E+15	4502686.8	4.5026868

Table 10. Input Parameters Used to Perform a Feasibility Analysis based on Subsided Revenue

ECONOMIC PARAMETERS	UNIT	VALUE		
		Minimum	Likliest	Maximum
Capital Cost	EUR/kW	2076	4209	6343
	US$/kW	2520	5110	7663.93
Capital Expenditure	US$	11,437,759.02	23,193,233.58	34,784,993.86
Operating Cost	US$/kWh	0.01	0.02	0.03
Revenue	TT/kWh	0.26	0.32	0.56
	US$/kWh	0.038	0.047	0.083

simulations in Crystal Ball for 100,000 trials, the probability of the geothermal project being able to generate more than 10% IRR is 11.292%. This IRR is not likely to occur due to this small probability. The probability of generating an IRR of 5% is 51.56%, which is considered to be a favorable probability for the project.

The factors impacting NPV that were investigated showed that the capital expenditure (CAPEX) had the greatest effect (-54.9%) on NPV in a negative way, while revenue from the project had the second highest, but positive effect (38.7%) on the project. This information shows that capital expenditure must be addressed in order for a project of this nature to become feasible.

Further investigation was done using revenue relating to other Caribbean countries where pricing for electricity was not as heavily subsidized by the state. This produced a more realistic result that proved more feasible for investment in a geothermal project. Referencing Table 10, relevant values were substituted for revenue and capital expenditure. The revenue value of US$0.35, which was the median typical cost of electricity in the Caribbean quoted by The Energy Chamber of Trinidad and Tobago [13], was incorporated into the study. An update of the capital expenditure value was also increased to US$40,593,233.58, which included the average completion cost of 6 wells within the geothermal model (EIA, 2016). The results showed that the project would have a payback in 2025 if the project were to begin in 2022. The NPV was calculated as US$98,583,371.64 and the IRR was 39.2% (Table 12). Utilizing realistic unsubsidized revenues reflect results that would be more favorable in making a case for investing in a geothermal energy project.

3.4. CO$_2$ Reduction Analysis

Geothermal projects, according to research, are claimed to be tremendously less impactful on the environment as opposed to fossil fuel energy generation projects. This section analyses the difference in the volume of carbon dioxide emitted through power generation using geothermal energy versus fossil fuels. In an attempt to determine realistic values, research was done on a paper by Bloomfield and Moore [30] that showed the potential pounds of CO$_2$ per kWh that can be expected from geothermal, coal, petroleum, and natural gas systems. The results of their study are shown in Table 13.

Values in Table 13 were crucial in the determination of CO$_2$ emitted from energy produced. This is also depicted in Figure 21. This graph illustrates that geothermal energy production produces far less CO$_2$ emissions when compared to fossil fuel energy sources. The reduction in CO$_2$ emissions from natural gas (the primary fossil fuel used to generate electricity in TT) to geothermal energy was 1043.07 MMlbs of CO$_2$ when using 4.19E+12 Btu of enthalpy over a 28-year period.

Table 11. Projected Payback, IRR and NPV from Economic Analysis

	UNIT	RESULTS
Payback	Year	2042
IRR	%	2.7
NPV	US$	-11,806,056.79

Table 12. Projected Payback, IRR and NPV from Economic Analysis

	UNIT	RESULTS
Payback	Year	2025
IRR	%	39.2
NPV	US$	98,583,371.64

4. Conclusion

This study showed how the distance between producers and injectors, as well as injection pressure, can impact the amount of enthalpy that can be produced. When well spacing was increased the cumulative enthalpy over the years of

Table 13. Emissions in Various Energy Source Departments [30]

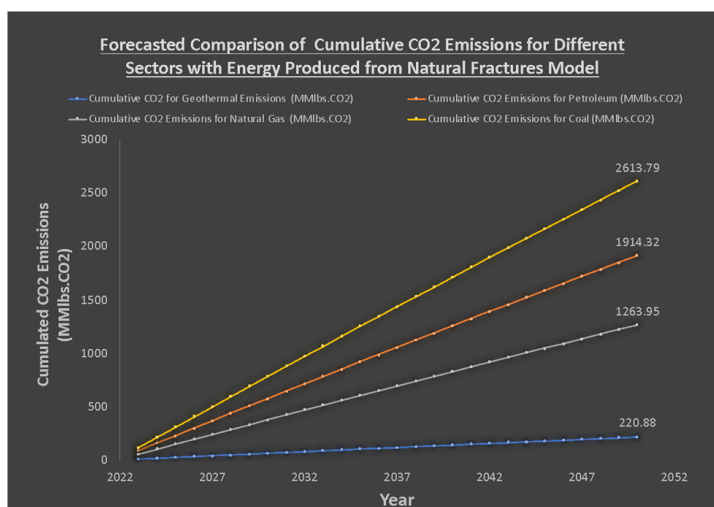|	Emissions (lbs.CO_2/kWh)
Geothermal	0.18
Coal	2.13
Petroleum	1.56
Natural Gas	1.03

Fig. 21. Forecasted Comparison of Cumulative CO_2 Emissions for Different Sectors with Energy Produced from Natural Fractures Model (3D Linear Elastic Model)

production also increased. Well spacing of 1300ft and a constant injection pressure of 1000psi reflected optimal results. When geomechanics was incorporated into the Natural Fractures 3D Linear Elastic model, it showed that 4.50 MW of power could potentially be generated. The project became more feasible when unsubsidized electricity rates were used as potential revenue. The results obtained showed that payback would occur in 3 years, IRR was 39.2%, and NPV was US$98,583,371.64.

There is an obvious dilemma regarding the reversal of the impact of climate change through the reduction of CO_2 emissions and the relatively low profitability of geothermal energy projects. In addressing this challenge, the Trinidad and Tobago government would need to intervene in several ways to provide incentives for companies to attain the levels of profit seen. The reduction of emissions by 1043.07 MMlbs of CO_2 when geothermal energy is used, as opposed to natural gas for the generation of electricity, should be enough to propel the leaders of this country to give serious thought to utilizing geothermal energy as one of its energy options.

References

[1] D. Indar, National energy efficiency monitoring report of Trinidad and Tobago, Project Documents, (LC/TS.2019/74), Santiago, Economic Commission for Latin America and the Caribbean (ECLAC), 2019.

[2] H. Ritchie and M. Roser, CO_2 and Greenhouse Gas Emissions, Published online at OurWorldInData.org. Retrieved from: https://ourworldindata.org/co2-and-other-greenhouse-gas-emissions, 2020.

[3] U.S. Energy Information Administration, EIA projects 28% increase in world energy use by 2040, Retrieved from: https://www.eia.gov/todayinenergy/detail.php?id=32912, 14 September 2017.

[4] M. Denchak, Greenhouse Effect 101, Published online at nrdc.org. Retrieved from: https://www.nrdc.org/stories/greenhouse-effect-101, 16 July 2019.

[5] GoRTT, Vision 2030 National Development Strategy 2016 – 2030, Ministry of Planning and Development, 2016.

[6] CEIC, Trinidad and Tobago Crude Oil: Production, Retrieved from: https://www.ceicdata.com/en/indicator/trinidad-and-tobago/crude-oil-production, 2021

[7] Y. Sun, M. Sun and X. Tang, "Influence Analysis of Renewable Energy on Crude Oil Future Market", 2019 IEEE 3rd International Conference on Green Energy and Applications (ICGEA), pp. 167-171, 16-18 March 2019.

[8] UNFCC, The Paris Agreement, United Nations Climate Change, Retrieved from: https://unfccc.int/process-and-meetings/the-paris-agreement/the-paris-agreement, 2020.

[9] A. Aktas, "A Review and comparison of renewable energy strategies or policies of some countries", 2015 International Conference on Renewable Energy Research and Applications (ICRERA), pp. 636-643, 22-25 November 2015.

[10] D. Icaza and D. Borge-Diez, "Potential Sources of Renewable Energy for the Energy Supply in the City of Cuenca-Ecuador with Towards a Smart Grid", 2019 8th International Conference on Renewable Energy Research and Applications (ICRERA), pp. 603-610, 3-6 November 2019.

[11] S. Z. Ilyas, A. Hassan and H. Mufti, "Review of the renewable energy status and prospects in Pakistan", In-

ternational Journal of Smart Grid, https://doi.org/hkk6, Vol. 5, No. 4, pp. 167-173, 2021.

[12] M. K. Mzuza and L. Sosiwa, "Assessment of Alternative Energy Sources to Charcoal in NTCHEU District, MALAWI", International Journal of Smart Grid, https://doi.org/hkk8, Vol. 5, No. 4, pp. 149-157, 2021.

[13] The Energy Chamber of Trinidad & Tobago, Understanding the Electricity Subsidy in T&T, Retrieved from: https://energychamber.squarespace.com/blog/understanding-the-electricity-subsidy-in-tt, 18 May 2017.

[14] IRENA, Geothermal energy, International Renewable Energy Agency, Retrieved from: https://irena.org/geothermal, 2021.

[15] R. Venegas, S. Kuravi, K. Kota and M. McCay, "Comparative Analysis of Designing Solar and Geothermal Power Plants: A Case Study", International Journal of Renewable Energy Research, https://doi.org/10.20508/ijrer.v8i1.6681.g7337, Vol. 8, No. 1, pp. 625-634, 2018.

[16] K. Rodrigues, Geothermal Hot Spots and Oil Occurrences Over Trinidad, The Geological Society of Trinidad & Tobago, 1989.

[17] A. Thomas, "The Hypothetical Cretaceous Petroleum System of Trinidad and Tobago", Geoscience Technology Workshop (GTW), Deep Horizon and Deep Water Frontier Exploration in Latin American and the Caribbean, 9-11 March 2014.

[18] E. Deville and S.-H. Guerlais, "Cyclic Activity of Mud Volcanoes: Evidences from Trinidad (SE Caribbean)", Marine and Petroleum Geology, https://doi.org/10.1016/j.marpetgeo.2009.03.002, Vol. 26, No. 9, pp. 1681-1691, November 2009.

[19] V. Ramlal, "Enhanced Oil Recovery by Steamflooding in a Recent Steamflood Project, Cruse 'E' Field, Trinidad", SPE/DOE Symposium on Improved Oil Recovery, 17-21 April 2004.

[20] GSTT, Geological Formations, Geological Society of Trinidad and Tobago, Retrieved from: https://thegstt.org/geoattract/formations, 2021.

[21] IRENA, Geothermal power: Technology brief, International Renewable Energy Agency, September 2017.

[22] E. Chekhonin, A. Parshin, D. Pissarenko, Y. Popov, R. Romushkevich, S. Safonov, M. Spasennykh, M. Chertenkov, V. Stenin "When Rocks Get Hot: Thermal Properties of Reservoir Rocks" Oilfield Review, Vol. 24, No. 3, Autumn 2012.

[23] G. Wilkinson, Water Properties, Thermopedia, DOI: 10.1615/AtoZ.w.water_properties, 2 February 2011.

[24] A. Villaluz, Relative Permeability of Fractured Rock, Stanford University, June 2005.

[25] T. Nguyen and K. Joslin, Geomechanics, Computer Modelling Group (CMG), 2020.

[26] H. Xu, W. Zhou, R. Xie, L. Da, C. Xiao, Y. Shan, H. Zhang "Characterization of Rock Mechanical Properties Using Lab Tests and Numerical Interpretation Model of Well Logs", Mathematical Problems in Engineering, https://doi.org/10.1155/2016/5967159, Vol. 2016, 16 May 2016.

[27] CMG, Geomechanics in CMG Software Tutorial, Computer Modelling Group (CMG), 2020.

[28] U.S. Energy Information Administration, Capital Cost and Performance Characteristic Estimates for Utility Scale Electric Power Generating Technologies, U.S. Department of Energy, February 2020.

[29] Office of Energy Efficiency and Renewable Energy, Geothermal FAQs, U.S. Department of Energy, Retrieved from: https://www.energy.gov/eere/geothermal/geothermal-faqs, 2020.

[30] K. K. Bloomfield and J. N. Moore, Production of Greenhouse Gases from Geothermal Power Plants, Geothermal Resource Council 1999 Annual Meeting, 17-20 October 1999.